Student thesis series INES nr 542

Evaluating the ability of LPJ-GUESS to simulate the tree size structures of tropical forests

Margot J. Knapen

2021

Department of
Physical Geography and Ecosystem Science
Lund University
Sölvegatan 12
S-223 62 Lund
Sweden

Margot J. Knapen (2021).
Evaluating the ability of LPJ-GUESS to simulate the tree size structures of tropical forests
Utvärdera förmågan av LPJ-GUESS att simulera trädstorleksstrukturer i tropiska skogar
Bachelor degree thesis, 15 credits in Physical Geography and Ecosystem Analysis
Department of Physical Geography and Ecosystem Science, Lund University

Level: Bachelor of Science (BSc)

Course duration: *March* 2021 until *June* 2021

Disclaimer

Evaluating the ability of LPJ-GUESS to simulate the tree size structures of tropical forests

---

Margot J. Knapen

Bachelor thesis, 15 credits, in Physical Geography and Ecosystem Analysis

Supervisor:
Thomas Pugh
Department of Physical Geography and Ecosystem Science,
Lund University

Exam committee:
Petter Pilesjö
Per-Ola Olsson
Department of Physical Geography and Ecosystem Science,
Lund University

ABSTRACT

Tropical forests are of great importance to all living-beings due to their high biodiversity and the valuable resources, such as food and fuel, they provide. In addition, tropical trees sequester a high amount of carbon and consequently over half of the global forest carbon stock can be found in the tropics. Climate change, however, might weaken this carbon sink and possibly result in tropical forests turning into net carbon sources. The tree size structures of forests and growth and mortality processes are strongly related to each other and determine the accumulation of biomass.

LPJ-GUESS is a Dynamic Global Vegetation Model (DGVM), which can be used to simulate tropical forest dynamics. However, it has not been thoroughly evaluated against field data of tropical tree size distributions. The aim of this study was therefore to further enhance our understanding of the behaviour of LPJ-GUESS by means of comparing simulated distributions of tree size versus tree density and tree size versus biomass to a validation dataset. Six locations within the tropical rainforest ecozone were chosen across Africa, South America and Southeast-Asia. It was found that LPJ-GUESS generally underestimates the total amount of biomass. A total of eleven parameters were adjusted according to the one-at-a-time principle, which showed large variability between the six sites. The results of the parameter changes are described and are consistent with expectations from the literature. An increase in the disturbance interval, for example, stimulated the accumulation of biomass whilst reducing the tree density. This can be explained by the fact that fewer disturbances cause trees to grow older and consequently store more biomass, whilst their bigger crowns reduce the amount of light passing through the canopy. Recommendations for further studies are presented and stress the importance of exploring parameters interactions. Based on the results from this study it is advised to explore the response of LPJ-GUESS when altering the disturbance interval, crown area and k_{allom1} (an allometric constant) simultaneously.

Table of Contents

List of abbreviations

Abbreviation	Description
AGB	Above-ground biomass
BR1	One of the study sites in South America (Brazil 1)
BR2	One of the study sites in South America (Brazil 2)
CA	Crown area
CMR	One of the study sites in Africa (Cameroon)
COG	One of the study sites in Africa (Congo)
d	Disturbance interval
DBH	Diameter at breast height
DGVM	Dynamic Global Vegetation Model
GPP	Gross primary productivity
$greff_{min}$	Minimum growth rate efficiency
IND	One of the study sites in Southeast Asia (Indonesia)
k_{allom1}	Allometric constant
k_{allom2}	Allometric constant
k_{allom3}	Allometric constant
k_{latosa}	Allometric constant
k_{rp}	Allometric constant
LA	Leaf area
LPJ-GUESS	Lund-Potsdam-Jena General Ecosystem Simulator
MYS	One of the study sites in Southeast Asia (Malaysia)
npatch	Number of patches
NPP	Net primary productivity
NSC	Normalized sensitivity coefficient
OAT	One-at-a-time
PFT	Plant functional type
SA	Sapwood cross-sectional area
SLA	Specific leaf area
SOC	Soil organic carbon
TEAM Network	Tropical Ecology, Assessment and Monitoring Network
TrBE	Tropical broadleaved evergreen tree
TrBR	Tropical broadleaved raingreen tree
TrIBE	Tropical broadleaved evergreen shade-intolerant tree
WD	Wood density

1 Introduction

At present approximately 31% of the terrestrial surface of the Earth is covered by forest, of which the largest part (45%) can be found in the tropical zone (FAO and UNEP 2020). The tropical zone is characterised by relatively high and stable temperatures (> 18°C) throughout the year, without any frost days (FAO 2012). Tropical forests can generally be divided into two categories: rainforest and monsoon (mixed) forest (Nair 2004). The main focus of this study is on tropical rainforests, which are primarily found at latitudes between the Tropics of Cancer and Capricorn (i.e. between 23°30'N and 23°30'S) and at an elevation of less than 1000 m (Adler 2013). Tropical rainforests are defined as a wet ecological zone, with a maximum of three dry months per year (FAO 2012).

Tropical forests are well-known for their high biodiversity, hosting a large variety of plant and animal species (Nias 2013). This biome is important from an economic perspective as it provides hundreds of millions of people with income, food and fuel (Zhou et al. 2013). In addition, tropical forests play a key role in the process of carbon sequestration. Roughly 55% of the global forest carbon stock can be found in tropical forests, of which the majority is stored as above-ground biomass (AGB) (Pan et al. 2011). Furthermore, over one-third of the global terrestrial net primary production (NPP) is accounted for by this biome (Phillips et al. 1998).

Tropical forests are of great importance for the global carbon cycle as they absorb more carbon than they release and can consequently be classified as a net carbon sink (Cramer et al. 2004). We know, however, that anthropogenic activities, such as commercial logging, can directly contribute to carbon loss to the atmosphere and therefore weaken this carbon sink (Mitchard 2018). In addition, the current and projected climate change might greatly affect the ability of forests to sequester carbon (Hubau et al. 2020). For the purpose of this study only intact tropical forests (i.e. without being disturbed by humans) have been taken into account.

A decrease in the sink strength has already been observed for the Amazonian forests and is predicted to occur for African forests in the near future (Hubau et al. 2020). The primary cause for the weakening sink is enhanced tree mortality (Brienen et al. 2015), for example due to drought stress (Aleixo et al. 2019) or increasing air temperatures (Locosselli et al. 2020). Yet, it remains highly uncertain to what extent the carbon balance in tropical ecosystems will be affected by the projected climate change. Understanding the dynamics of tropical forests is consequently of great importance.

One factor that can have a substantial impact on the ability of tropical forests to store carbon is their structure (Muller-Landau et al. 2006). The number of trees by size, usually expressed as the diameter at breast height (DBH), is commonly referred to as the tree size distribution (Farrior et al. 2016). Large tropical trees (DBH ≥ 70 cm) account for a considerably higher share of the stored carbon (Chave et al. 2001) and accumulate carbon more rapidly than smaller trees (Stephenson et al. 2014).

Dynamic Global Vegetation Models (DGVMs) are frequently used to simulate biomass stocks and carbon fluxes of forests (Ostle et al. 2009). DGVMs capture the properties of and interaction between vegetation and the soil. Simulations based on future climate scenarios can be run which provides valuable information on the possible impact of climate change. In order to reduce the uncertainty of the simulations, model evaluation by means of field data is required (Ostle et al. 2009). For this particular study, LPJ-GUESS (Lund-Potsdam-Jena General Ecosystem Simulator) was used (Smith et al. 2014). LPJ-GUESS can simulate gap dynamics, unlike many other DGVMs (Pugh et al. 2020). A more detailed description of this model can be found in section 2.2.

In principle, LPJ-GUESS is able to capture the size structures of tropical forests, but the results from the simulations have not been evaluated for this region. Some regional studies in the tropics have been conducted, for example by Seiler et al. (2015) who applied an adapted version of LPJ-GUESS to simulate the transition from evergreen to deciduous forest in Bolivia. Further studies are also necessary to gain a better understanding of the sensitivity of the simulated size structures when key processes, such as tree mortality and competition between different functional strategies, are altered.

1.1 Aim of study

The aim of this study is threefold:

1) Evaluating the current state of LPJ-GUESS against field data of tropical tree size structures on a pan-tropical scale (South America, Africa and Southeast Asia).
2) Gaining a better understanding of the driving factors behind tropical forest dynamics through a sensitivity study of parameters related to growth and mortality in LPJ-GUESS.
3) Identifying the most prominent shortcomings when LPJ-GUESS is used for tropical forest modelling and proposing additional actions to improve its overall accuracy.

Key words: tropical forests, tree size distributions, LPJ-GUESS, carbon, biomass, sensitivity analysis

2 Methods

2.1 General overview

The methodology that has been applied in this study is summarized in *Figure 1*. A more detailed description of LPJ-GUESS, the validation data used and the approach for the final analysis is provided in the upcoming sections of this chapter.

As can be seen in *Figure 1* the first step was to clean the validation data and to compare this to the output generated by running LPJ-GUESS with its default parameter values. The next step was to run

the model with adjusted parameters according to the one-at-a-time (OAT) approach. Parameter screening was conducted and seven parameters were chosen for further analysis. Additional simulations were run and the output was analysed and compared with the default simulation. A sensitivity analysis was performed by means of the normalized sensitivity coefficient (NSC) and differences between the simulations and validation data were investigated. Based on the results from the analyses a number of recommendations for further studies were proposed.

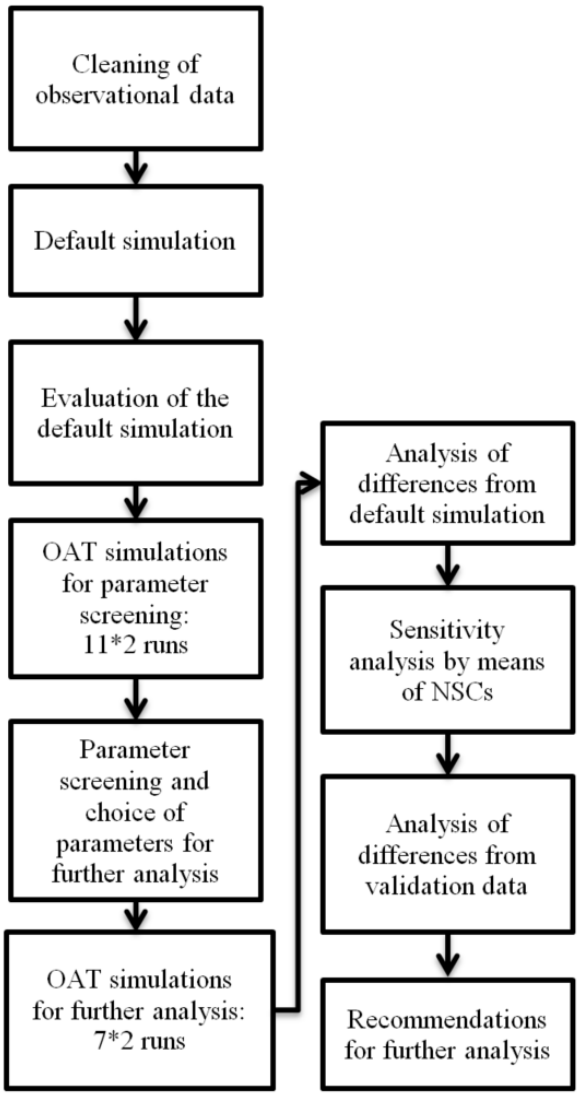

Figure 1. Flow chart visualizing the methodology applied in this study.

2.2 The LPJ-GUESS dynamic global vegetation model

The DGVM that was used in this study was LPJ-GUESS version 4.0 (Smith et al. 2001; Smith et al. 2014). The description of the model given in the upcoming subchapters refers to Smith et al. (2014) unless otherwise stated.

2.2.1 Model description

LPJ-GUESS can be used to simulate vegetation dynamics on both a regional and global scale. The state of the modelled ecosystem is affected by a variety of processes, some of which are accounted for on a daily and others on an annual basis. *Figure 2* lists the most important processes and components of the ecosystem state. The input that the model requires consists of data on climatic conditions (temperature, precipitation and incoming radiation), the concentration of atmospheric CO_2 and soil type. This version of LPJ-GUESS also includes plant and soil nitrogen dynamics.

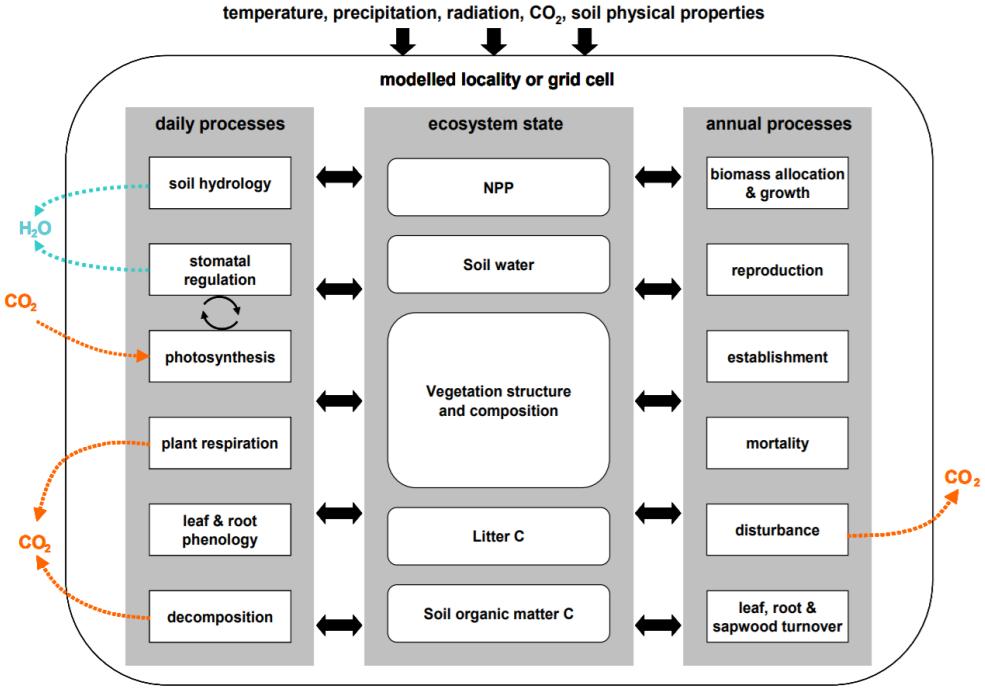

Figure 2. A schematic overview of the most important daily (fast) processes and annual (slow) processes that are accounted for in LPJ-GUESS. This figure is taken from (Smith n.d.).

Forests are generally composed of a large variety of tree species and their characteristics can vary considerably. This is why all individuals are grouped into plant functional types (PFTs) that have certain similarities, for example in leaf phenology or bioclimatic niches. The standard version of LPJ-GUESS consists of three tropical PFTs (see *Table 1*), which have been used in this study. One of the main characteristics of a tropical PFT is that the trees can only survive when the minimum air temperature is 15.5 °C or higher.

Table 1. The three tropical plant functional types (PFTs) used in this study.

PFT	Leaf phenology	Shade tolerance
TrBE	Evergreen	Tolerant
TrIBE	Evergreen	Intolerant
TrBR	Raingreen	Intolerant

The geographic extent of a simulation is represented by a specific grid cell of 0.5°x0.5°. The model simulates the woody plants and herbaceous undergrowth, which is affected by competition for resources. The simulation for each grid cell consists of a specific number of replicate patches, which each have a size of 0.1 hectare, in order to capture the different states found across the landscape and to account for this by taking the average of the replicate simulations.

When running the model there is initially no established vegetation present. The first step is the spin-up time phase where repeated, detrended 1901-1930 climate data is applied along with the CO_2 concentrations for the year 1901 and N deposition rate. The vegetation is allowed to grow from bare ground. Once an equilibrium, or "steady-state", has been obtained the simulation moves on to the historical phase. This second phase uses observed, and often interpolated, climate and CO_2 data.

2.2.2 Model set-up

LPJ-GUESS was run using cohort mode which implies that all individuals belonging to the same age class and PFT are identical and represented by an average individual. The default values for the total number of replicate patches and spin-up phase were used, which were 100 and 1200 years respectively. Initially simulations were run using 25 patches, but this proved to be too low as the simulated output tended to fluctuate considerably. Increasing the number of patches (*npatch*) to 100 resulted in more stable simulations (see *Figure A* in *Appendix A*). The climate data and CO_2 concentrations used in the historical phase ranged from 1901 to 2015 (Le Quéré et al. 2016).

2.3 Validation data and data cleaning

The validation data that was used for this study has been acquired from the Tropical Ecology, Assessment and Monitoring (TEAM) Network (2021) and was pre-processed as part of the TreeMort project (2021) to add information on height and biomass based on allometric equations. Data was available for a total of 15 sites covering the years 2002-2017. Each site comprised six or more 1 hectare plots. The data provided information on both individual tree and plot level, a selection of which was used in this study (see *Table 2*).

Table 2. Metrics from the validation dataset that were used in this study.

Tree level	Plot level
Diameter	Carbon loss
Height	Carbon production
Biomass	Stem loss rate

The validation data on biomass was given as above-ground biomass (AGB) in Mg/ha whereas the simulated values also included carbon stored by the roots and was given in kgC/m^2. Both were converted to give the biomass as AGB in kgC/m^2. The simulated biomass was multiplied by 0.75 to account for the biomass stored by the root system and to consequently approximate the AGB (Penman et al. 2003). The observed biomass from the validation data was multiplied by 0.5 to obtain the tree carbon content (Saatchi et al. 2011).

For the purpose of this study six locations have been used to evaluate the output of LPJ-GUESS. Due to substantial regional differences between the dynamics of tropical forests (Blundo et al. 2021) a cross-continental approach was deemed appropriate. Africa, South America and Southeast Asia were each represented by two study sites, see *Figure 3*. The locations were chosen such that the region's predominant ecozone, as defined by the FAO (2012), was either classified as tropical moist forest or tropical rainforest.

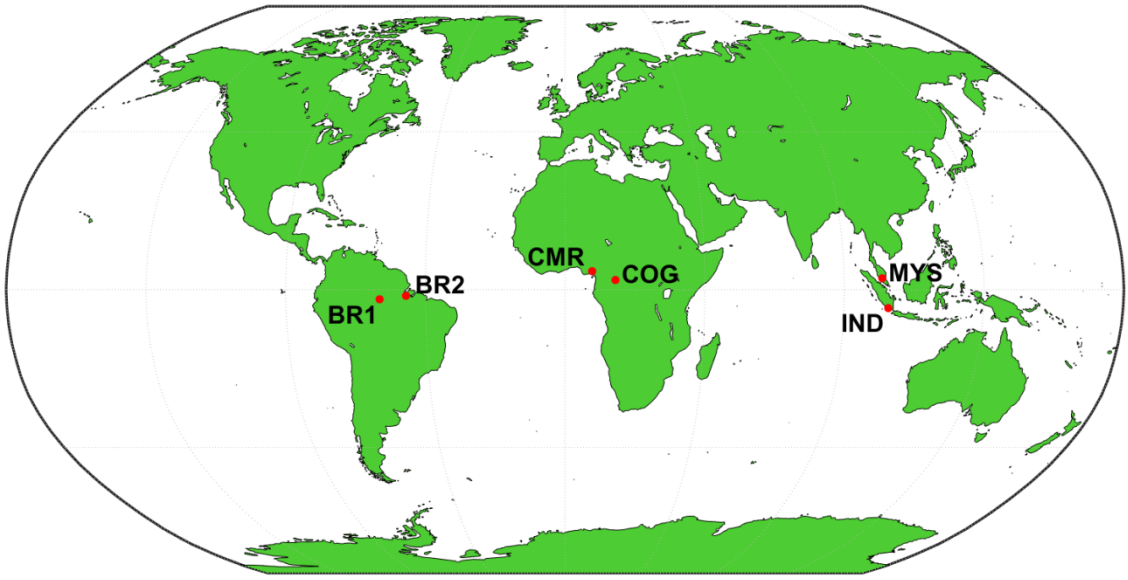

Figure 3. Map illustrating where the six sites are located.

For each site data from one single year was used, the choice of which depended on the availability of valid data on both tree and plot level. The dataset contained various errors, but for the data on tree level years could be chosen without any invalid entries, see *Table **3***. However, data cleaning was necessary for the data on plot level as this was calculated based on the data from the individual trees. At IND, for example, there were approximately 100 observations of trees with a DBH of 999 cm indicating that no data was available. One tree at MYS was assigned a DBH of 2401 cm, which was considered to be unlikely high and thus invalid. Some plots had extremely high values for carbon production and carbon loss and, despite thorough examination of characteristics of the individual trees, no obvious errors could be found. In order to make sure that unlikely values were not included in the analysis, all entries with a carbon production of more than 20 Mg/ha/yr were excluded, as this was considered to be the maximum (Malhi et al. 2011).

The data from the TEAM Network provided information on the longitude and latitude of the plots. The coordinates for the six sites have then been approximated to the nearest of 0.5°x0.5° grid cell for which climate data was available.

Table 3. Overview of the described characteristics of each site. Note that the latitude and longitude refer to the values used as input for LPJ-GUESS and consequently differ from the exact location of the sites.

Site	Country	Year	Plots	# trees	# plot entries	Latitude	Longitude
COG	Congo	2014	1-6	2053	20	2.75	16.25
CMR	Cameroon	2011	1-6	2879	6	5.25	8.75
BR1	Brazil	2011	1-6	3749	42	-2.75	-59.75
BR2	Brazil	2014	1-6	2789	67	-1.75	-51.25
IND	Indonesia	2012	1-6	2594	18	-5.25	104.25
MYS	Malaysia	2015	1-3, 7-9	3116	13	3.25	102.25

2.4 Parameterization

2.4.1 Parameter estimation

After the model had been run with the default values for all input parameters, some parameters were adjusted using a one-at-a-time (OAT) approach. This implied that all parameters were held at their default values whilst one was varied. A total of eleven parameters were analysed, which are listed in *Table 4* and discussed in more detail below.

Trees, being primary producers, fix carbon dioxide (CO_2) through photosynthesis and allocate part of this captured energy to respiration and growth. The net primary productivity (NPP) can be deduced from the gross primary productivity (GPP) after accounting for the plant respiration (Ngoma et al. 2019). The NPP allows for tree growth as it is distributed to the leaves, sapwood and fine roots on an annual basis. The exact portion that each of these three living tissue pools receive, depends on a number of constraints which are largely influenced by the allometric constants in LPJ-GUESS (Smith et al. 2014). There are three key allometric equations governing the relations of stem diameter, height, crown area and leaf area, each will be investigated here. In addition, key parameters related to tree mortality will be discussed: the disturbance interval, minimum growth efficiency and tree longevity.

The relation between the crown area and the diameter of the stem is described as (Smith et al. 2014):

$$CA = k_{allom1} \cdot D^{k_{rp}} \quad (1)$$

where *CA* is the crown area, *D* the stem diameter and k_{allom1} and k_{rp} are constants. Crown area is limited to a specific maximum value (CA_{max}) that cannot be exceeded. The initial value of CA_{max} used in LPJ-GUESS was 50 m^2. Several studies indicate, however, that this should be considerably more.

Seiler (2014) conducted a study on the tropical forests of Bolivia and adjusted the maximum crown area to 650 m^2. By means of an airborne inventory, Herwitz et al. (2000) found a maximum crown area of about 365 m^2. Kuntoro et al. (2009) distinguish between "primary dominant" and "primary non-dominant" trees, which were determined to have a maximum crown area of 300 m^2 and 15 m^2 respectively. It was deemed likely that CA_{max} had to be increased in order to more realistically capture the dynamics of tropical forests. Yet, given the information acquired from the study by Kuntoro et al. (2009), a simulation with $CA_{max} = 15\ m^2$ was run as well (*Table 4*).

The study by Seiler (2014) proposed an increase of k_{allom1} from 250 to 374. For primary dominant trees Kuntoro et al. (2009) suggested a more moderate increase ($k_{allom1} = 300$), whilst Braakhekke et al. (2019) applied a lower value ($k_{allom1} = 166$). Kuntoro et al. (2009) stated that primary non-dominant trees should be assigned an even lower value of $k_{allom1} = 100$. Given the wide range of the previously stated figures, initially two simulations were run with $k_{allom1} = 100$ and $k_{allom1} = 300$.

The diameter of a tree increases as it grows taller, which is largely influenced by two allometric parameters (k_{allom2} and k_{allom3}) according to:

$$H = k_{allom2} \cdot D^{k_{allom3}} \tag{2}$$

Equation (2) is usually solved for *D* when *H* has been deduced from:

$$H = \frac{c_{sap} \cdot k_{latosa}}{\rho_{sap} \cdot c_{leaf} \cdot SLA} \tag{3}$$

where c_{sap} is the sapwood mass, k_{latosa} a constant, ρ_{sap} the sapwood density, c_{leaf} the leaf mass and *SLA* the specific leaf area.

Kuntoro et al. (2009) suggested $k_{allom2} = 60$, which was the same as the default value in LPJ-GUESS Version 4.0, and $k_{allom3} = 0.92$. Seiler (2014) applied lower values for both constants ($k_{allom2} = 36$ and $k_{allom3} = 0.58$) whereas Braakhekke et al. (2019) proposed $k_{allom2} = 41.1$ and $k_{allom3} = 0.84$. To gain a further understanding of the impact and importance of these constants, the values were adjusted from 30 to 80 for k_{allom2} and from 0.35 to 1 for k_{allom3}.

A tree allocates a certain amount of its NPP to the sapwood, which allows for the transportation of water to the leaves. The relation between the sapwood cross-sectional area (*SA*) and the maximum individual leaf area (*LA*) is given as (Smith et al. 2014):

$$LA = k_{latosa} \cdot SA \tag{4}$$

where k_{latosa} is a constant which was originally set at 6000 for broadleaved trees. Kuntoro et al. (2009) used a value of 9000 for primary dominant trees and 3000 for primary non-dominant trees, both of which have been applied in this study.

Tree mortality occurs as a result of a variety of processes and events, such as fire and stress related to unfavourable climatic conditions. An important component is also the competition between individuals as a result of scarcity of vital resources such as water and light. Three parameters that directly influence the mortality rate in LPJ-GUESS were altered: disturbance interval (*d*), $greff_{min}$ and longevity. In cohort mode, patches are affected by randomly occurring disturbances that cause the death of all its individuals. The disturbance interval indicates the likelihood (*1/d*) of a disturbance taking place and was originally estimated to be 100 years. Seiler (2014) increased the interval and found that a value of 200 years represented the Bolivian forests most realistically as this increased the amount of stored carbon whilst still allowing for gap dynamics necessary for the growth of deciduous trees. To evaluate the effect of altering the disturbance interval on a cross-continental basis, rather than a regional one, values ranging from 100 to 600 years were used in this study.

Trees with low growth efficiency, defined as the ratio of NPP to leaf area index, are more likely to die as a result of stress. This component of tree mortality is accounted for in LPJ-GUESS by the parameter $greff_{min}$, which indicates the minimum growth efficiency necessary for survival. An individual has a 30% likelihood of death if its five-year average growth efficiency drops below the assigned value for $greff_{min}$ (Smith et al. 2001). The values assigned to $greff_{min}$ were increased and decreased by 50%, implying a range from 0.02 to 0.06 for shade-tolerant species and 0.06 to 0.1 for shade-intolerant species.

The age of trees is restricted in LPJ-GUESS by the PFT-specific parameter tree longevity. Only a few trees can live longer than the assigned longevity value. The three tropical tree PFTs are characterized by a different longevity. Based on the default values, the shade-tolerant PFT (TrBE) can reach an age of 500 years, whereas this is limited to 200 years for TrIBE. Tree longevity can vary substantially between species and as a result of climatic conditions. A recent study estimated the average longevity of tropical trees to be 186 ± 138 years, implying a shorter life-span than measured in boreal and temperate regions (Locosselli et al. 2020). However, the maximum age of tropical trees can largely exceed this mean value. Condit et al. (1995) used mortality rates to estimate the longevity and found a maximum value of 2000 years. This study was, however, criticized by Worbes and Junk (1999) who stated that tree longevity is commonly over-estimated and that the actual maximum tree age is likely to be between 400 and 500 years. A study by Fichtler et al. (2003), on the other hand, mentioned a slightly higher value of 600 years. Given the indefinite information provided in literature, it was deemed relevant to try a number of different values for tree longevity. The parameter was adjusted, for one PFT at a time, to both 50% higher and 50% lower values than the default.

Table 4. An overview of the parameters that were altered and used for the OAT simulations.

Parameter	PFT	Default	Modified values	Unit
CA_{max}	All trees	50	15 – 650	m^2
k_{allom1}	All trees	250	100 – 400	(-)
k_{allom2}	All trees	60	30 – 80	(-)
k_{allom3}	All trees	0.67	0.35 – 1	(-)
k_{latosa}	All trees	6000	3000 – 9000	(-)
disturbance interval	All trees	100	200 – 600	years
$greff_{min}$	Shade-tolerant	0.04	0.02 – 0.06	$kgC/m^2/yr$
$greff_{min}$	Shade-intolerant	0.08	0.06 – 0.1	$kgC/m^2/yr$
longevity	TrBE	500	250 – 750	years
longevity	TrIBE	200	100 – 300	years
longevity	TrBR	400	200 – 600	years

2.4.2 Screening of the parameters

Due to the limited amount of time and the complexity of parameter interactions, not all parameters were studied equally thoroughly. Initially LPJ-GUESS was run for both the minimum and maximum value of each parameter as mentioned in *Table 4*. The simulated values for the total number of trees and the total biomass were plotted. Parameter changes that showed a large range were considered more important and were consequently used for further analysis.

2.5 Sensitivity analysis

For the parameters that were selected after the previously mentioned screening method had been conducted, two additional simulations were run. The parameter values were chosen such that they were in between the default and the extremes (i.e. minimum and maximum as listed in *Table 4*) or, as was the case for the disturbance interval, in between the two extremes. The normalized sensitivity coefficient (*NSC*) was calculated, given as:

$$NSC = \frac{|Y - Y_0|}{|X - X_0|} \cdot \frac{|X_0|}{|Y_0|} \tag{5}$$

where X_0 and Y_0 are the nominal parameter and output values respectively, X the altered parameter value and Y the output when running the model with X (Hou et al. 2015). The *NSC* is a positive number which provides information on how sensitive the model is when run with a particular altered parameter value. Several studies use a threshold of $NSC < 0.1$ to define insensitive parameters, but this is said to be rather subjective (Duru et al. 2009; Hou et al. 2015).

The NSC is, across different fields of studies, a quite commonly used local sensitivity method which indicates the importance of parameter changes (Chung et al. 2009; Pavurala and Achenie 2013). How-

ever, from the NSC it is not possible to derive whether the adjusted parameter has a positive or negative impact on the model. For this reason, the difference between the default simulation and the output of each OAT simulation were also compared.

2.6 Evaluation of the simulated output

The sensitivity analysis gives valuable information on the behaviour of LPJ-GUESS to parameter changes. However, from the NSCs one cannot deduce how well the simulations correspond to the validation data. In order to account for this, the simulated tree density and total biomass were compared to the validation data, according to:

$$measure\ of\ goodness = \frac{Y_{obs}}{Y_{sim}} \cdot 100\% \quad (6)$$

where Y_{obs} indicates the mean observed value and Y_{sim} the output generated by the model. The calculations were repeated for all parameter values at each of the six sites. The results were then visualized by means of heat maps where the outcome of each parameter change per site is given.

3 Results

3.1 Observations

The provided validation data contained observations on the diameter, height and biomass of individual trees. *Table 5* lists the total number of trees per hectare and the biomass observed at the six locations. Large tree biomass refers to the biomass that is accounted for by trees with a DBH of 70 cm or more. There is considerable variability across the plots at each site, as expressed by the minimum and maximum values. It is also apparent that as mean tree density increases, the average large tree biomass decreases.

Table 5. Observed tree density, biomass and biomass accounted for by large trees (DBH ≥ 70 cm) at the six sites. Mean values have been calculated by taking the average of the six plots that each site comprises. Min. and max. refer to the range observed across the plots.

	Tree density (trees/ha)			**Biomass (kgC/m^2)**			**Large tree biomass (%)**		
Site	**Mean**	**Min.**	**Max.**	**Mean**	**Min.**	**Max.**	**Mean**	**Min.**	**Max.**
COG	342	269	400	21.0	12.2	27.2	55	25	89
CMR	489	390	613	17.7	11.6	23.4	30	0	61
BR1	625	588	676	16.0	13.6	19.9	10	0	26
BR2	465	424	506	22.9	17.2	25.8	36	18	44
IND	432	245	516	14.2	7.9	21.8	40	9	84
MYS	519	338	670	13.7	10.4	17.3	23	5	65

For each site the average carbon production, carbon loss and stem loss rate were calculated from the plot-level statistics provided in the dataset, the results of which are presented in *Table 6*. There was no data on carbon loss and stem loss rate available for CMR. For the other sites a rather similar carbon production and loss can be observed, although the forest stand at IND has a considerably more pronounced carbon loss.

Table 6. Mean observed carbon production, carbon loss and stem loss rate for the six sites.

Site	Carbon production ($kgC/m^2/year$)	Carbon loss ($kgC/m^2/year$)	Stem loss rate (%)
COG	0.51	0.18	1.98
CMR	0.48	-	-
BR1	0.56	0.20	1.22
BR2	0.53	0.21	1.18
IND	0.57	0.01	0.14
MYS	0.50	0.19	2.46

3.2 Initial state of the model

Figure 4 shows both the tree density that was observed and simulated using the default parameter values for each of the six sites. The average observed tree density was calculated by taking the mean of each site's six plots and the variety between the plots is illustrated by the error bars which indicate the standard deviation.

With regard to the observation data, COG, BR1 and BR2 show relatively low variation across the plots as indicated by the modest error bars. BR1 has the highest tree density whilst the number of trees per hectare is lowest at COG. The default simulations generally result in a lower tree density than the mean of the observed values, especially at BR1 and MYS.

The observed (mean) and initial simulated biomass are depicted in *Figure 5* where the height of the bars indicates the total biomass and the grey parts show the biomass accounted for by the large trees. *Figure 5* visualizes the previously mentioned statement that as the tree density increases, the large tree biomass at the observation sites decreases (see also *Figure B* in *Appendix B*). This does, however, not seem to be as consistent for the simulated biomass distribution. The simulated large trees at BR1, for example, store more carbon than at CMR, even though BR1 has the highest simulated tree density.

Overall the default simulation results in a considerable underestimation of the total biomass for the sites in Africa (COG and CMR) and South America (BR1 and BR2). The simulated biomass at IND,

on the other hand, is higher than the observed values. At MYS the model output is rather similar to the mean observed biomass, but it should be noted that this site has a large variability across the six plots.

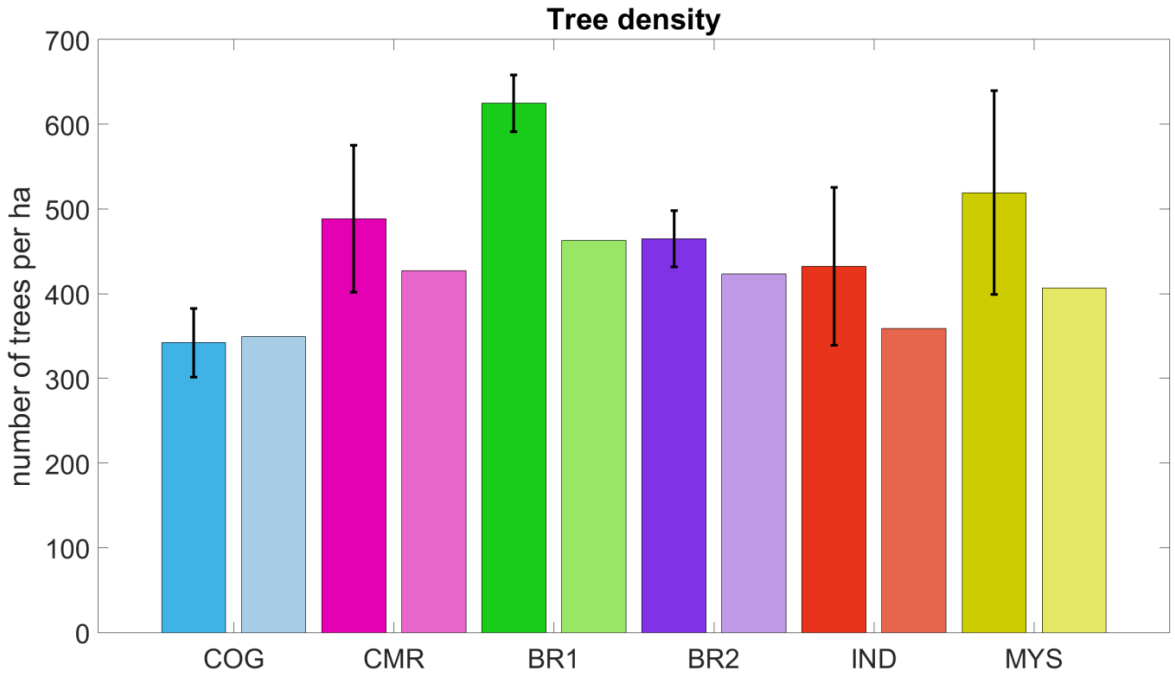

Figure 4. Number of trees per hectare at the six sites, where both the mean observed tree density (left, darker shades) and the results of the default simulation (right, lighter shades) are shown as pairs indicated by similar colours. Error bars for the observed tree density indicate the standard deviation calculated based on the six plots at each site.

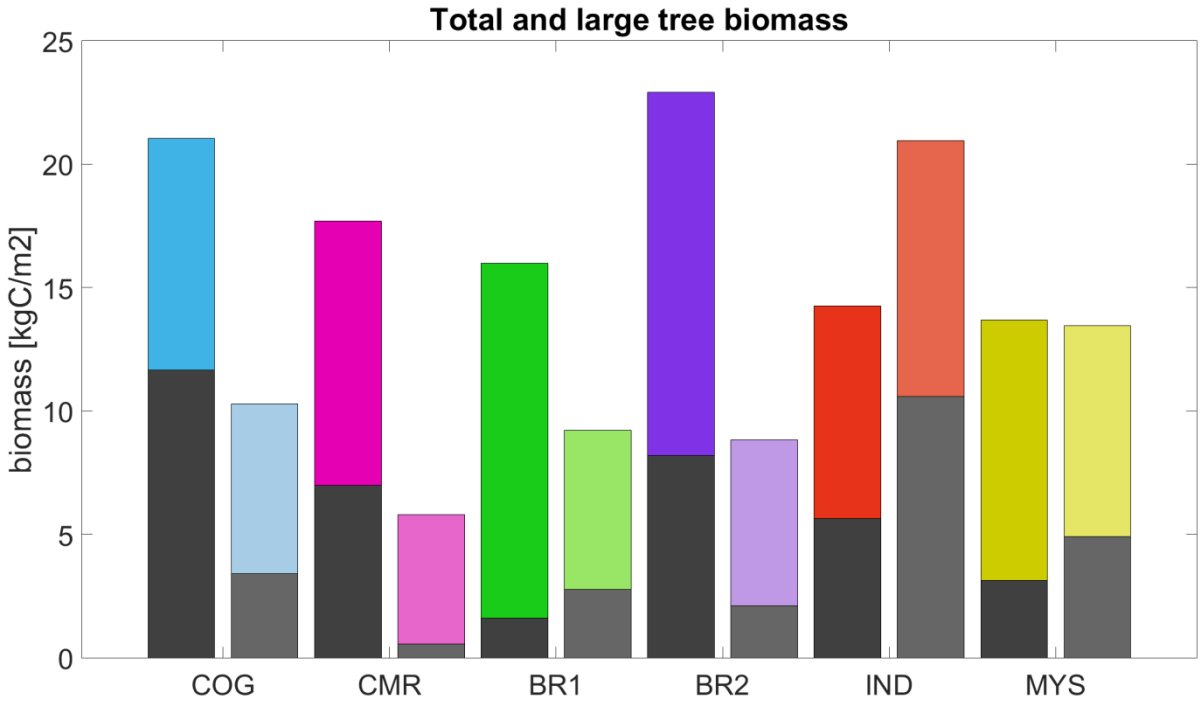

Figure 5. Biomass per site where the average of the six plots has been taken at each site. The grey parts indicate the biomass accounted for by the trees with a DBH of more than 70 cm. Observations are shown in darker shades.

Figure 6 gives an overview of the size distributions of the forests, based on the relative number of trees per size class, for both the validation data and the default simulation. At all sites the percentage of trees within the smallest size category (10-20 cm) are overestimated by the model, except for IND. At IND the default simulation results in a distinct overestimation of large trees. The size distribution at COG is striking in the sense that there is a large overestimation of trees within the smallest size class which seems to reduce the share of 20-30 cm and 30-40 cm trees.

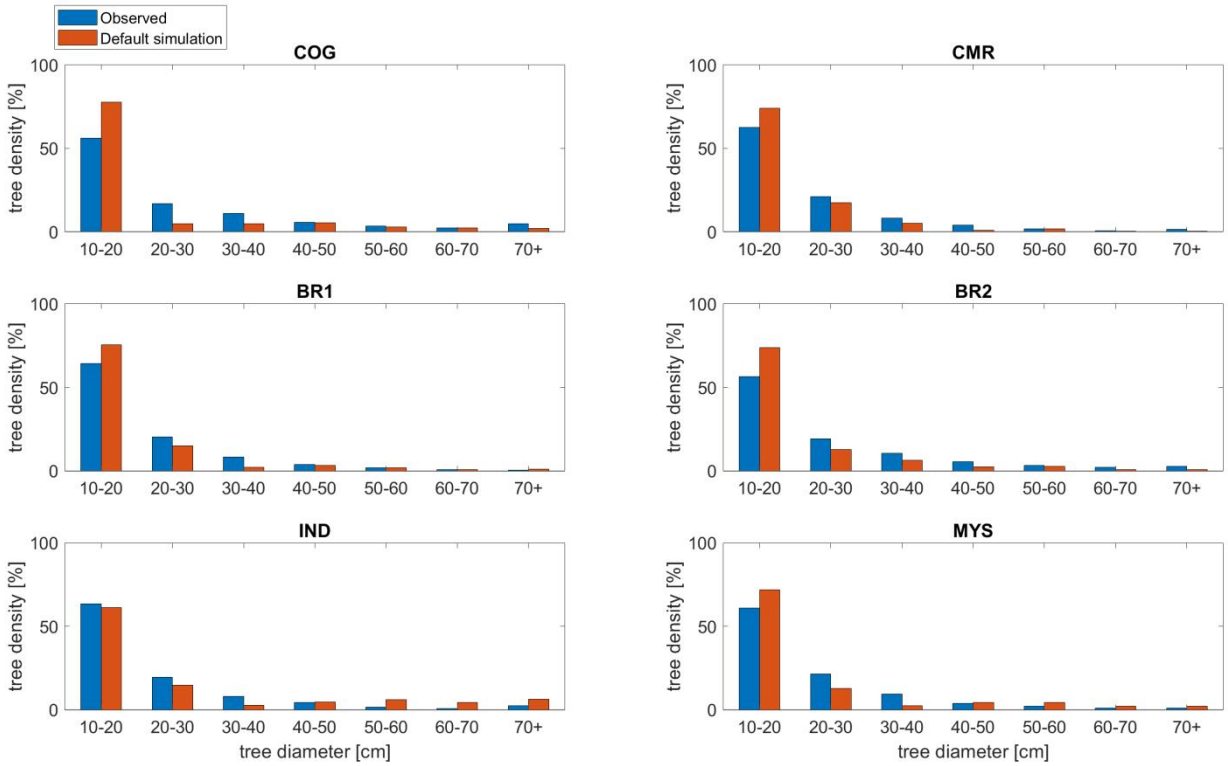

Figure 6. Relative number of trees (i.e. number of trees as a percentage of the total number of trees) grouped into seven diameter classes (cm).

3.3 Parameter screening

Figure 7 and *Figure 8* illustrate the response of the model on tree density and biomass when it was run with the two adjusted values (see *Table 4*). The different colours indicate the six plots and the length of the bars are a measure of the model's response to the altered parameter. Striking is the large variability between the sites, with some sites appearing to be more sensitive than others. The biomass at IND is, for example, affected largely by several parameters whereas the impact on the other sites is less pronounced.

Based on the results presented in *Figure 7* and *Figure 8*, the model seems least sensitive to CA_{max}, k_{allom3}, *longevity TrIBE* and *longevity TrBR*. These parameters are, therefore, not used in the more detailed analysis of this study. More specifically this decision was made by visual interpretation taking the variability and extent of the responses into account. The criteria to include or discard a certain parameter were made divided into three parts:

1) Does the parameter result in a clear response for all sites (e.g. k_{latosa})?
2) Are there any distinct exceptions (e.g. IND for longevity TrBE)?
3) Does the parameter change appear to cause a distinct higher or lower output (e.g. biomass for the disturbance interval)?

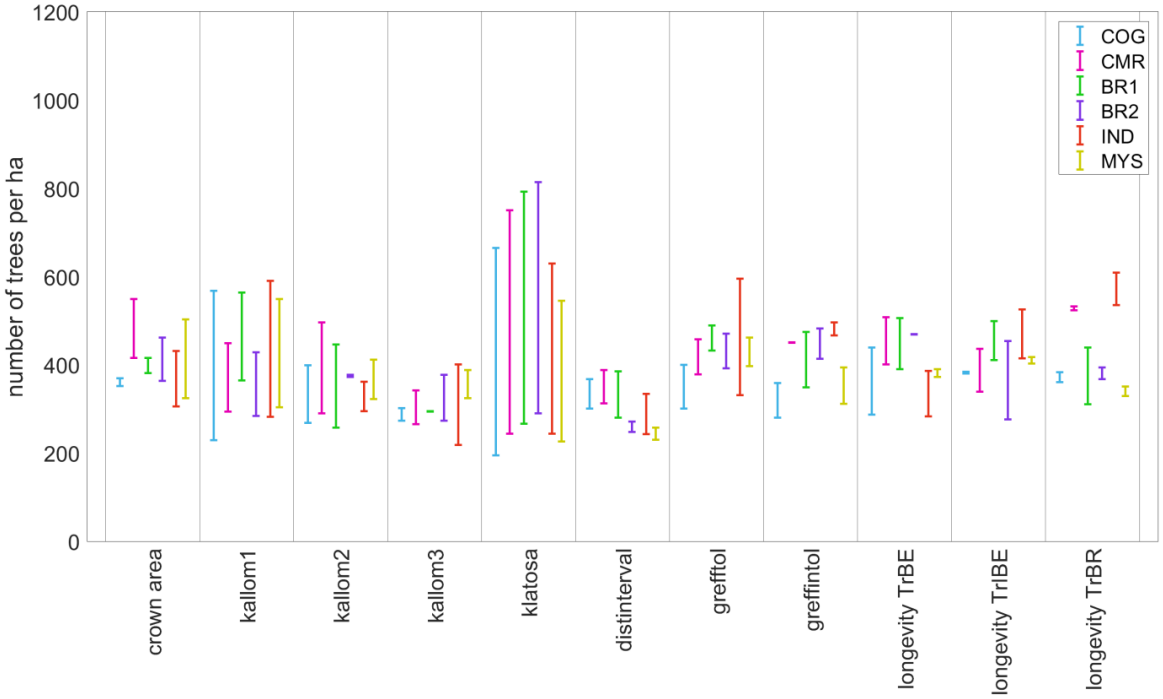

Figure 7. Response of the altered parameters, with the maximum and minimum values as listed in Table 4, on the tree density.

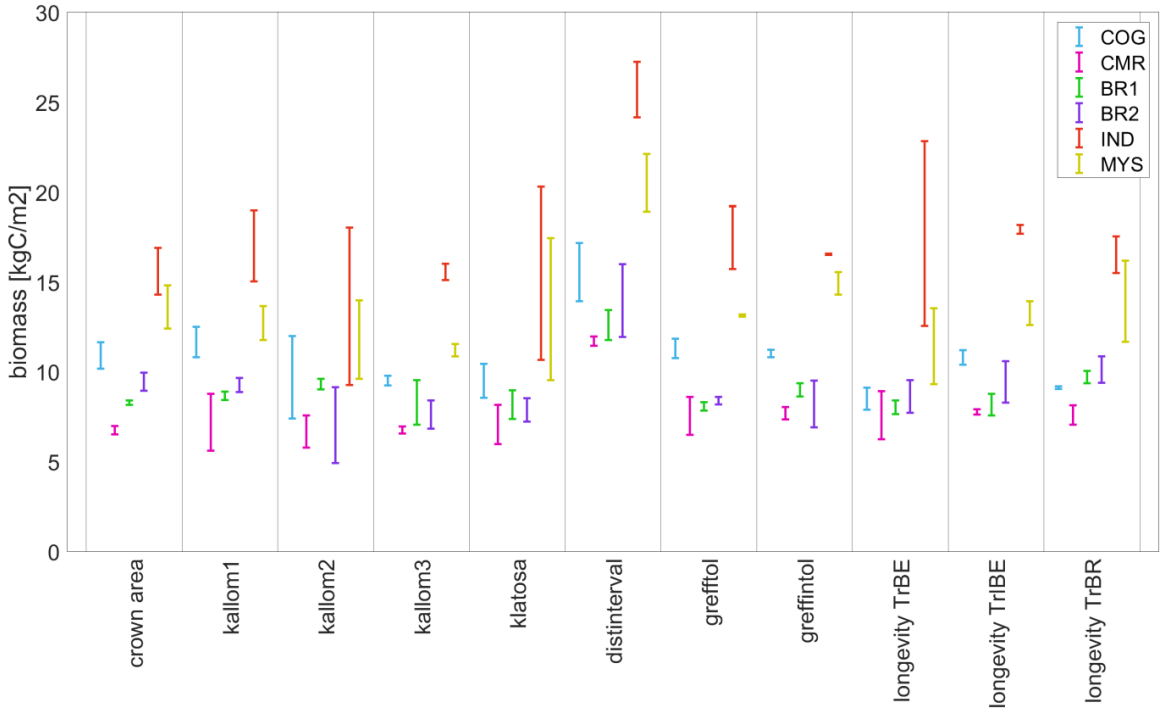

Figure 8. Response of the altered parameters, with the maximum and minimum values as listed in Table 4, on the total biomass.

3.4 Parameterization

Note that abbreviations of the parameter names are used in the figures presented in the upcoming sections. The parameter values are given in parentheses.

The model was run four times for all seven parameters that were chosen according to the previously described screening method. The results are presented by means of heat maps which illustrate the relative difference between the default simulation and the output from each OAT run.

Figure 9 depicts how the simulated tree density is affected by the parameter changes. Striking is the large increase in the number of trees per hectare when reducing k_{latosa} to 3000. Reducing k_{allom1} also appears to stimulate an increased tree density. When lowering k_{allom2}, on the other hand, a reduction in the tree density can be observed. The same is true for increasing k_{latosa} and the disturbance interval. Adjusting $greff_{min}$ and the longevity of TrBE appears to alter the tree density to a lesser extent and in a rather inconsistent manner. Changing these parameters seems to affect IND more than the other sites.

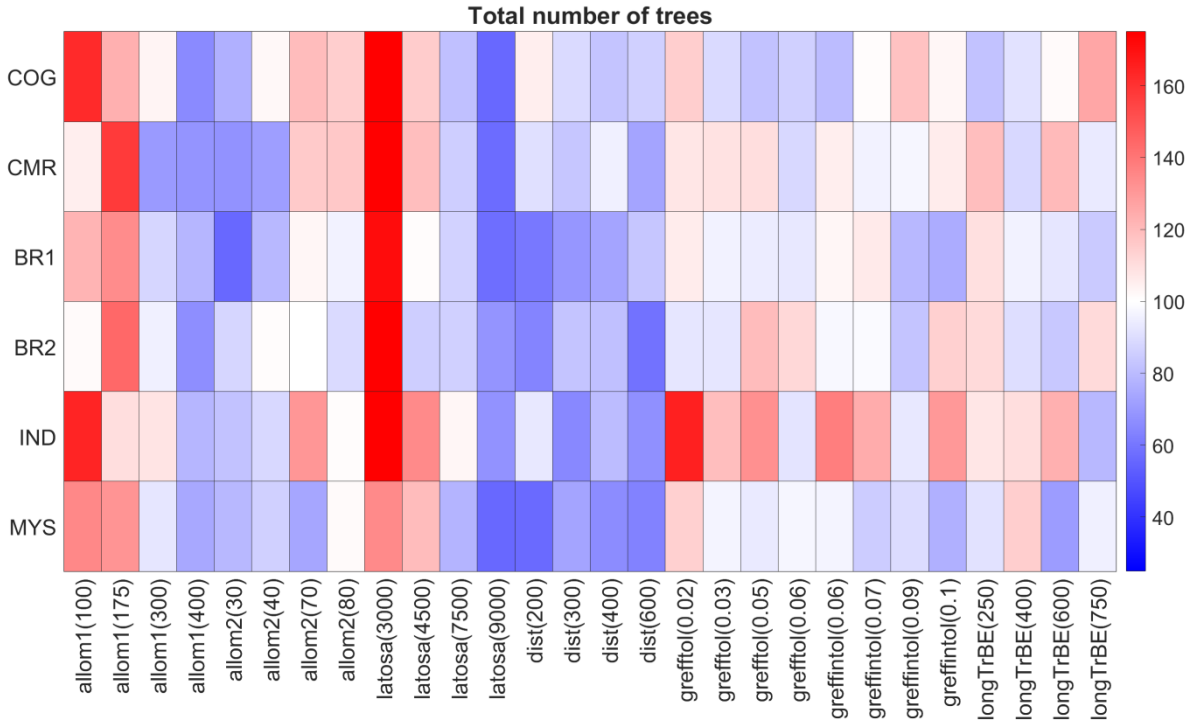

Figure 9. The relative tree density compared to the default simulation, where red tiles indicate a higher simulated tree density for the OAT run than for the default.

The differences in biomass are illustrated in *Figure 10*. The large number of red tiles indicates that the parameter changes tend to cause an increase of biomass at CMR, whilst decreases are more commonly observed at IND. An enhanced accumulation of biomass can be observed for all sites when increasing the disturbance interval, although this is least pronounced at IND. A decrease in total biomass occurs when lowering k_{allom2} or increasing k_{latosa}.

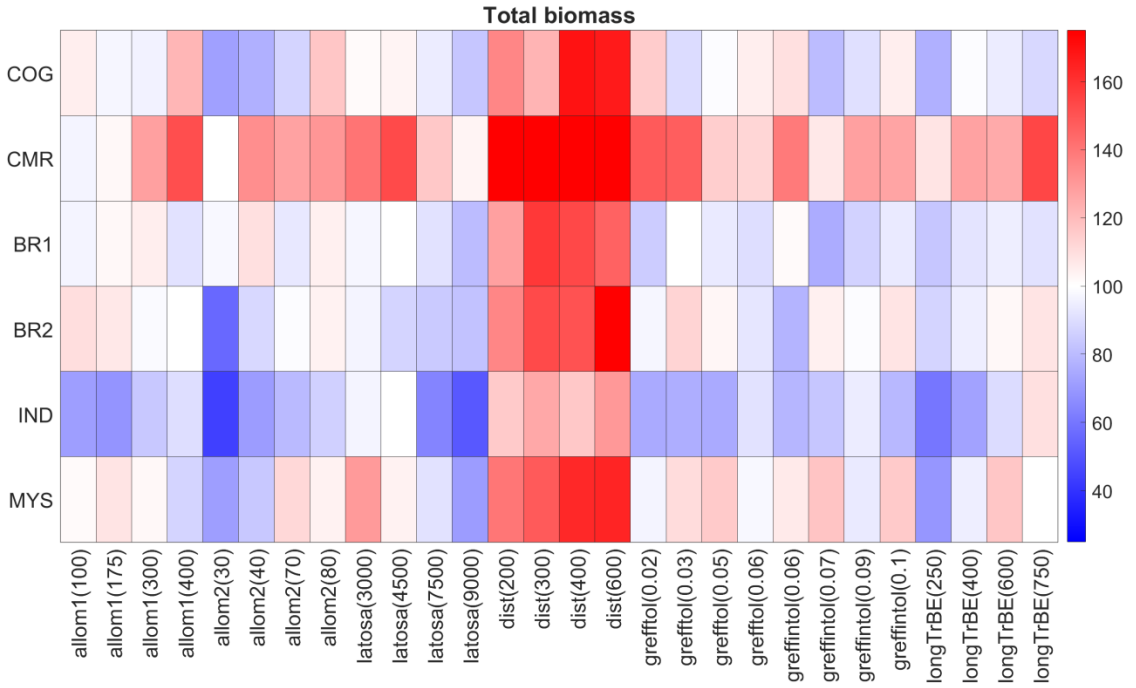

Figure 10. The relative total biomass compared to the default simulation, where red tiles indicate a higher simulated biomass for the OAT run than for the default.

In order to gain a better understanding of how the adjusted parameters influence forest composition, the simulations were run with three PFTs, with one being shade-tolerant (TrBE) and the other two shade-intolerant (TrIBE and TrBR). *Figure 11* shows the relative number of shade-tolerant trees (i.e. the number of TrBE trees divided by the sum of all trees).

For most parameters and the default simulation, about 50% of all trees are shade-tolerant. However, there are some exceptions. Shade-intolerant trees seem to be favoured in conditions with a low k_{allom1}, low k_{allom2} or a high k_{latosa}. An increase in shade-tolerant trees can primarily be observed for a decrease in k_{latosa} or increase in the disturbance interval.

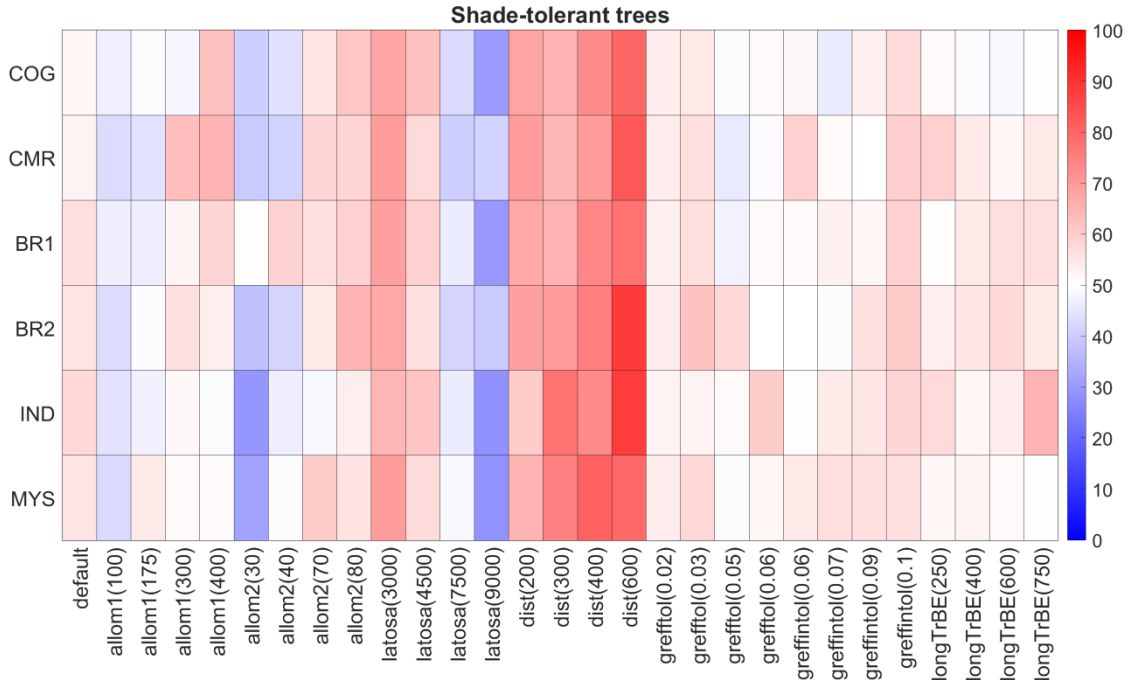

Figure 11. Relative number of TrBE (shade-tolerant) trees, where red tiles indicate an abundance of shade-tolerant trees whilst blue tiles imply a large share of shade-intolerant (TrIBE+ TrBR) trees.

3.5 Normalized sensitivity coefficient

The results of the sensitivity analysis are presented in *Figure 12 a*nd *Figure 13*, where the NSC for each site and each adjusted parameter value is plotted. The differences between the sites are clearly depicted by the wide range of NSCs for certain parameters. The tree density NSC for $k_{allom1} = 175$, for example, varies from approximately 0.3 to 2. The model behaved in a rather similar way for some other parameters as, for instance, $k_{allom1} = 400$ resulted in NSCs for tree density fluctuating between 0.35 and 0.57. In general, the model appears to be highly sensitive for the majority of the parameter changes at CMR and IND.

There are a number of parameter changes that the model seems to be rather insensitive to, primarily with regard to the tree density. The most distinct examples of this are $greff_{min} = 0.06$ for shade-tolerant PFTs and TrBE longevity of 750 years. A disturbance interval of 200 years generates NSC values of maximum 0.5, which is, in comparison to many of the other parameter changes, rather low. A striking exception is the biomass NSC at CMR, which is approximately equal to 1. In general, the model's sensitivity declines as the disturbance interval is further increased.

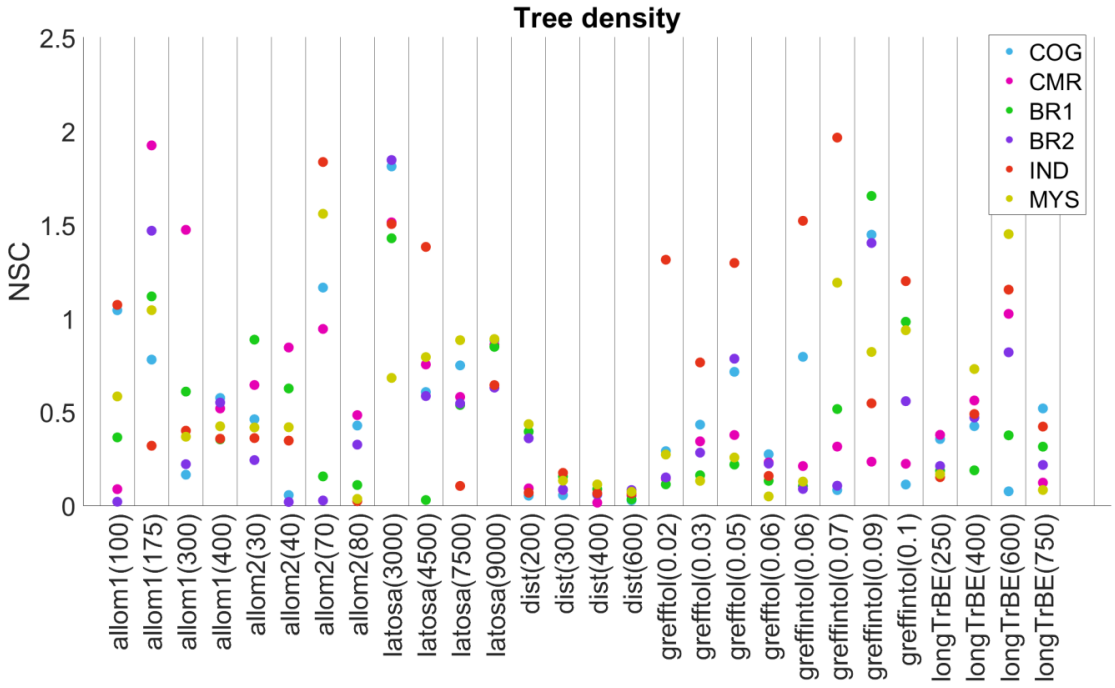

Figure 12. NSCs for tree density calculated based on the adjusted parameters where each dot with a similar colour represents a specific site.

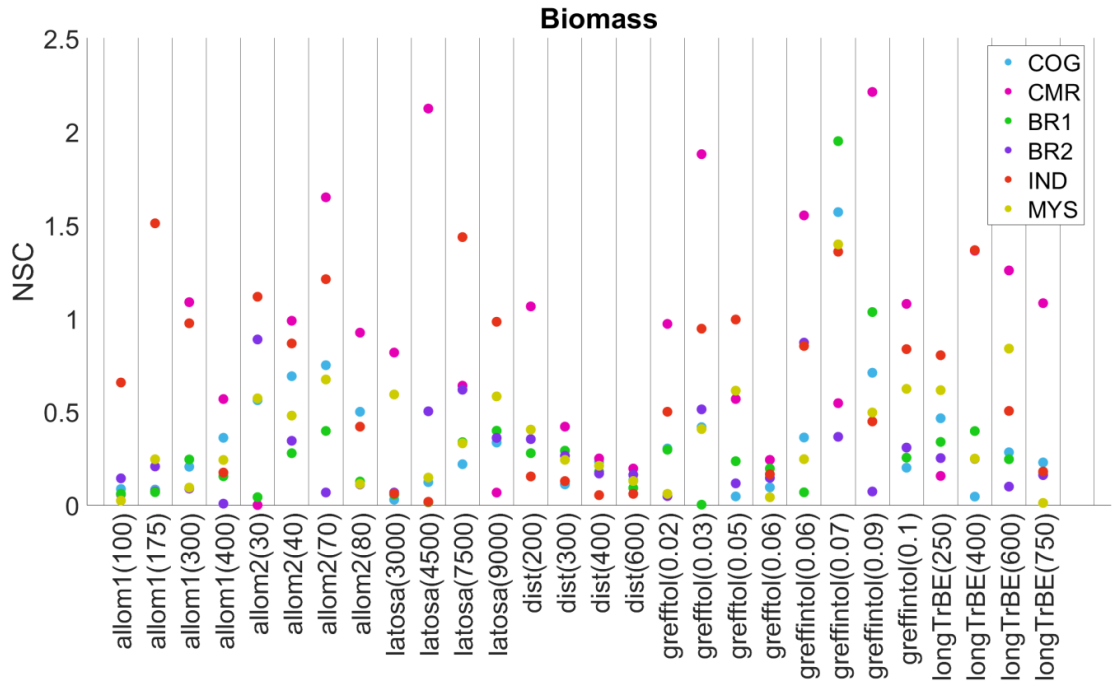

Figure 13. NSCs for total biomass calculated based on the adjusted parameters where each dot with a similar colour represents a specific site.

3.6 Comparison with validation data

Figure 14 shows how the simulated tree density relates to the observations obtained from the validation data. The latter is defined as the mean number of trees per hectare taken from the six plots at each site. The first column depicts the output when running the model with the default parameter values. As in accordance with *Figure 4*, initially there is a slight overestimation at COG and underestimations for all other sites.

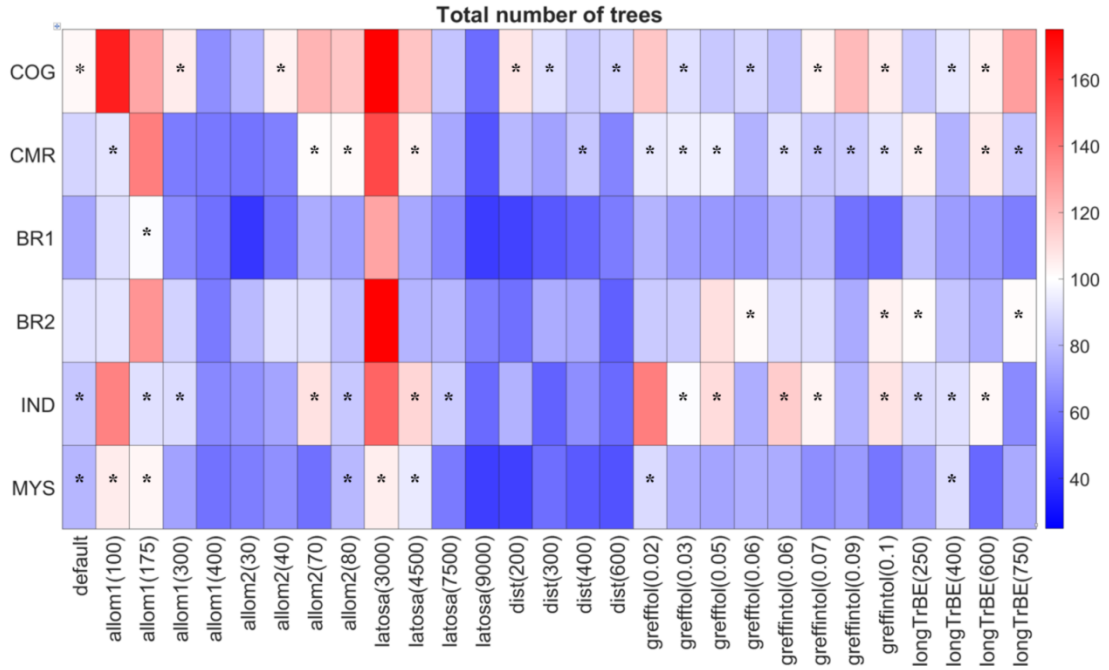

*Figure 14. Heat map illustrating the simulated tree density relative to the mean observed tree density. Blue tiles indicate an underestimation of the model, whilst overestimates are represented by red tiles. A * indicates that the output was within the range of the observed tree density according to the validation data.*

Figure 15 shows the total biomass of the simulations relative to the mean observed biomass in a similar manner as *Figure 14*. Striking are the predominant blue tiles for the two African (COG and CMR) and South American (BR1 and BR2) sites, which indicate that the model vastly underestimates the total biomass. The increase in disturbance interval results in a higher total biomass, which is an improvement for the sites in Africa and South America. For IND and MYS, on the other hand, this implies that the simulated biomass exceeds the mean observed biomass. Reducing k_{allom2} and longevity TrBE both lead to a lower total biomass, just as increasing k_{latosa} to 9000.

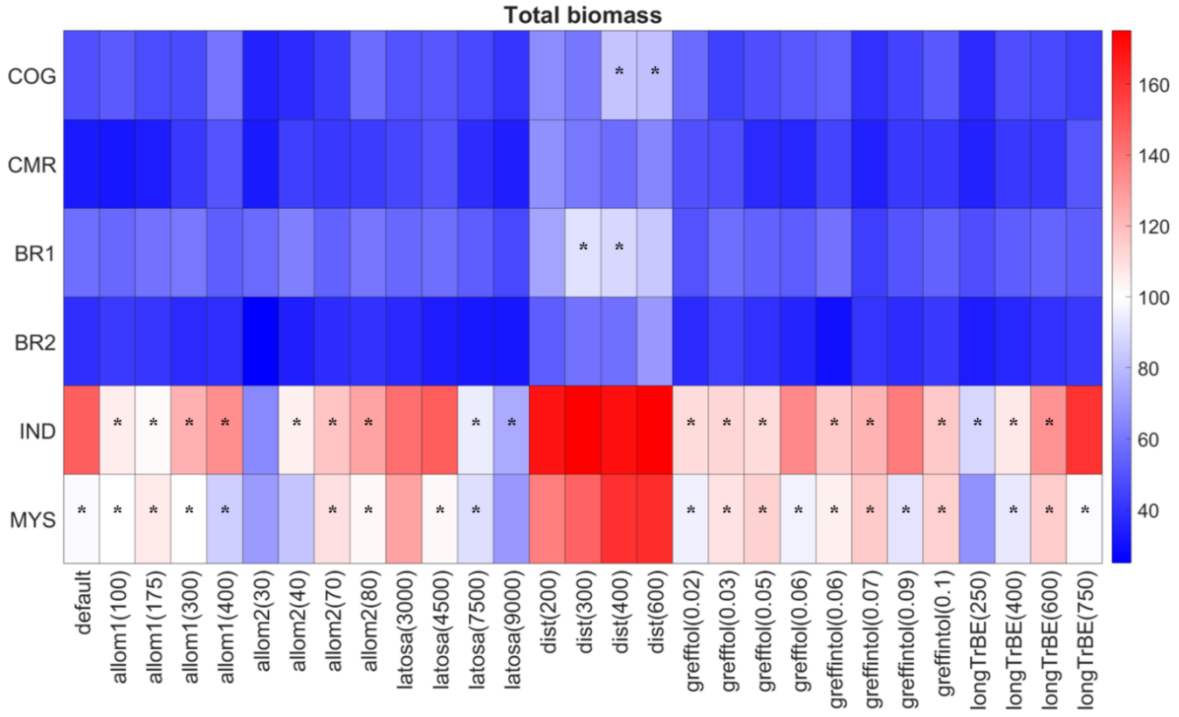

*Figure 15. Heat map illustrating the simulated total biomass relative to the mean observed total biomass. Blue tiles indicate an underestimation of the model, whilst overestimates are represented by red tiles. A * indicates that the output was within the range of the observed biomass according to the validation data.*

4 Discussion

This section aims to explore possible reasons behind some of the most striking observations, uncertainties and differences that were presented in *Results*. It is subdivided into three main parts which each relate to one of the aims of this study.

4.1 Observations and the default simulation

From the validation data on individual tree level it can be observed that BR1 has the highest tree density and the lowest large tree biomass, whereas this is the opposite at COG. This is in accordance with literature and is caused by a process called self-thinning (Westoby 1984). Trees compete with each other to obtain the necessary resources (water, light and nutrients) which ultimately leads to the death of the weakest individuals. Young forests are generally characterized by a combination of a high number of trees per hectare and low total biomass. As the tree density increases, resources become more scarce and a shift towards an ecosystem with fewer but larger trees can be observed (Pillet et al. 2018). This is an indication that the forest stand at BR1 could be younger than at COG.

At all sites the validation data indicates that the production is much higher than the loss of carbon. There does not appear to be a clear linkage between the mortality rate and accumulation of biomass,

which could be caused by the limited temporal resolution. It might imply that no extreme disturbances have occurred during the census years. Data on carbon production and loss ranging over a longer period of time might, therefore, considerably affect the results.

The simulation using the default parameter values of LPJ-GUESS resulted in an underestimation of biomass at all sites. The only exception was IND where both the total and large tree biomass was considerably higher than what one would expect based on the validation data. Especially the default simulation for biomass at IND is peculiar, given the underestimations at the other sites. The tree density and relative number of shade-tolerant trees do not appear to differ in an equally extreme manner. I hypothesize that IND differs from the other sites as a result of the soil characteristics. The soil at IND is richer in nitrogen (N) and soil organic carbon (SOC) than at the other sites (de Sousa et al. 2020). For means of comparison, the top 5 cm of the soil at IND contains about 350 cg/kg N and 800 dg/kg SOC whereas this is only 210 cg/kg and 280 dg/kg, respectively, at BR1. In addition, the soil at IND is not as sandy (28%) as at BR1 (40%) (de Sousa et al. 2020). Sandy soils enhance the leaching of N (Smith et al. 2014). The soil at CMR is composed of about 70% of sand which might contribute to the limited accumulation of biomass. The deviating results obtained for IND might be related to the N cycle that is incorporated in LPJ-GUESS.

4.2 Parameterization and sensitivity analysis

The impact of decreasing k_{allom1} on the tree density and PFT distribution is consistent for all sites and indicates an increase in tree density and a larger number of shade-intolerant trees. These observations might be due to a smaller crown area which enables more light to pass through the canopy. This in turn would favour the fast-growing shade-intolerant trees which can quickly result in a dense forest. Another possibility would be that the leaves get packed into a relatively small space which would limit light to pass through. In extreme cases this could imply that even shade-tolerant species cannot establish. Increasing k_{allom1} generally lowers the tree density, but does not appear to cause a distinct decline in shade-intolerant species, the exception being the two African sites, where about 60% of the simulated trees are shade-tolerant for $k_{allom1} = 400$. Besides this increase of roughly 10% in TrBE trees, the biomass is also considerably higher at COG and CMR.

When decreasing the value for k_{allom2} the tree density declines and more shade-intolerant trees emerge. This might be due to increased competition for light as a result of smaller trees with bigger crowns. According to equation (2) a bigger diameter is needed to reach a given height. The total biomass drops as well, except for at CMR and BR1. At these two sites the decline in tree density is the most pronounced and thus this relatively high amount of biomass is a result of more large trees. A biomass reduction is observed for the other sites due to fewer trees per hectare, but no clear increase of large trees. Shade-intolerant trees might be favoured as a result of their higher SLA (Seiler 2014). Gap dynamics might also play an important role in the PFT-distribution as the death of a wide tree could in-

crease the amount of light reaching the ground which would make it possible for shade-intolerant trees to establish.

Altering k_{latosa} results in simulations that are distinctly different from the default run. A reduction from 6000 to 3000 greatly stimulates tree density and 65-70% of the trees are shade-tolerant. An increase to 9000 implies a vast decline in the number of trees and the dominance of shade-intolerant species. The total biomass is slightly increased when $k_{latosa} = 3000$, whereas a pronounced decline can be observed when $k_{latosa} = 9000$. This could be explained by the fact that leaves get packed more closely together which would cause less light to pass through the canopy and might thus favour the shade-tolerant trees. Another explanation can be deduced by means of equation (4). Increasing k_{latosa} might cause a higher leaf area to sapwood area ratio (LA:SA), which in turn is associated with taller trees that have a bigger diameter and crown area (Kuntoro et al. 2009). However, there is a decline in biomass which appears contradictory. A possible explanation for this observation is that the shade-intolerant PFTs are favoured as their sapwood turnover rate is higher and are consequently more apt to survive in conditions with a high LA:SA ratio. Another potentially important phenomenon is that a higher LA:SA ratio might result in less NPP going into the wood as it is instead distributed to the leaves.

Increasing the disturbance interval resulted in a lower tree density, more shade-tolerant trees and an increase in biomass. This can be justified given that these adjusted conditions make it possible for trees to grow into larger and older trees. Yet, based on the NSC, the model appears to be rather insensitive to the disturbance interval whilst a considerable increase in biomass was observed at all six sites. This can be explained by the fact that the relative increase for the disturbance interval (from 100 years to 200-600 years) is much higher than for the other adjusted parameters and consequently produces a rather low NSC.

Altering $greff_{min}$ yielded overall rather moderate and inconsistent changes for both shade-tolerant and shade-intolerant PFTs. One possible explanation could be that the current climate is favourable for the survival of the trees. This would imply that, as long as the climatic conditions remain stable, the trees are less likely to die due to limited growth efficiency.

Tree longevity does not appear to have a major impact on the simulated tree density and biomass. This might be due to the rather low default disturbance interval of 100 years. This causes relative frequent large-scale mortality events which might prohibit trees from reaching the longevity threshold.

4.3 Further studies

4.3.1 Additional parameters

A large variety of parameters were adjusted in this study, but LPJ-GUESS comprises many more. One of the constants that has not been altered but is included in allometric equation (1) is k_{rp}. Some studies on tropical forest modelling propose a slightly lower value (Seiler 2014; Ngoma et al. 2019), which would imply smaller trees with bigger crowns and consequently a lower tree density.

Another parameter that is quite commonly adjusted for tropical studies is the wood density (*WD*), which influences the tree diameter. The value of *WD* varies greatly among different tree species, which one would ideally account for (Phillips et al. 2019). Numerous studies indicate that the default value of 200 kgC/m^3 is too low for tropical trees (Reyes et al. 1992; Kohyama et al. 2003; Sabah Forestry Department 2013; Ngoma et al. 2019). Seiler (2014), on the other hand, proposed more modest changes with a slight reduction for TrIBE. Worth to note is also that trees with a low wood density are more likely to die as a result of drought (Phillips et al. 2010).

4.3.2 Improved validation data

One of the main limitations encountered while conducting this study was the poor quality of the validation data. The observations at individual tree level were cleared from obvious erroneous data points according to the criteria described in section 2.3. It was considered too time-consuming to verify all entries and therefore some errors might not have been detected. Yet, the main problem lies with the data on plot level. The validation dataset was pre-processed and the individual trees were used to derive values for the growth and mortality processes on plot level. This implies that it was not possible to account for the erroneous entries that were removed during the data cleaning phase on individual tree level. Drawing any clear conclusions on tree growth and mortality processes was for most sites not possible due to too few data points. The two exceptions were BR1 and BR2 which had 42 and 67 entries, respectively.

A direct comparison between the growth processes for the validation data and the simulations could not be made as the model lacked information on the woody growth rate. Writing a code to include this in LPJ-GUESS could greatly enhance our understanding of the model's response to the adjusted parameters, but was omitted due to time limitations.

The PFT distribution as shown in *Figure 11* gives valuable information on how the parameter adjustments affect the composition of a tropical forest. The validation data did include tree species on the individual tree level, but to classify these to fit the three PFTs would be extremely challenging given the limited available trait information for tropical forests, which made a direct comparison between the simulation and validation data impossible. Furthermore, it should be noted that, due to the structure of

available model outputs, the simulated tree density per PFT included trees with a diameter of 0-10 cm, whereas this size class is excluded for all other analyses in this study.

4.3.3 Parameter interactions

The OAT method that was applied in this study has provided information on the sensitivity of the individual parameters. However, this approach is simplistic as parameter interactions are neglected. In order to account for this, further studies where multiple parameters are adjusted simultaneously are necessary. Statistical analysis could be done by means of ANOVA and the Sobol' methodology can be applied to investigate the model's sensitivity (e.g. Pappas et al. 2013).

Based on the results obtained through this study, one of the most interesting combinations of parameters would be CA_{max} and k_{allom1}. Recall that an increase in k_{allom1} resulted in more biomass at the two African sites (COG and CMR), but a slight reduction was observed at the other four sites. I hypothesize that this is due to the limit set for CA_{max}. Equation (1) states that an increase in k_{allom1} would reduce the tree diameter, when $CA = CA_{max}$. This would reduce the number of large trees and, given their importance in carbon sequestration, limit the total simulated biomass. Yet, an increase in biomass can be observed for COG and CMR which might indicate that CA_{max} is not reached. Instead the crown area increases which leads to a high number of shade-tolerant trees.

A third parameter that would be interesting to include in a study on parameter interactions would be the disturbance interval. Despite the considerable increase necessary, and consequently the low NSC, it is the only parameter that seems to get somewhat close to observed biomass obtained from the validation data for the African and South American sites. It does, however, largely overestimate the biomass at the two Asian sites and the tree density is too vastly reduced. This could imply that the disturbance interval should be adjusted on a regional, rather than a global, scale.

Another interesting combination of parameters would be the disturbance interval and tree longevity. In this study, the tree longevity for TrBE was increased to a maximum of 750 years, whilst keeping the disturbance interval at 100 years. The likelihood of a tree actually reaching 750 years under such conditions is rather small. Rerunning the model with an increased tree longevity and disturbance interval might cause a higher number of large trees.

5 Conclusions

Limited studies have been conducted on the ability of LPJ-GUESS to model tree size structures in the tropics. This study aimed at evaluating the current state of the model by comparing simulated tree density and biomass against field data on a pan-tropical scale (South America, Africa and Southeast

Asia). It was found that the model is quite good at simulating the tree density, but underestimates the biomass at most sites.

In order to understand the behaviour of LPJ-GUESS eleven parameters related to tree growth and mortality were altered using a one-at-a-time approach. The simulated tree density, biomass and PFT composition were analysed and a local sensitivity analysis using the normalized sensitivity coefficient was conducted. This showed that the model is sensitive to most parameter changes, although there was a high variability between the six sites. The parameters that caused the most distinct changes were the allometry constants k_{allom1}, k_{allom2} and k_{latosa}. A decrease in k_{allom1}, for example, implied a higher tree density which could be explained by a smaller crown area or more leaves being packed in a small space. Parameters that the model was less sensitive to are $greff_{min}$ and tree longevity. This could be due to the low disturbance interval.

This study concludes with a number of remarks related to further studies. The most important component would be to explore the impact of altering multiple parameters at the same time. Parameter combinations that are recommended to be used are k_{allom1}, CA_{max} and the disturbance interval or the tree longevity and the disturbance interval.

6 References

Adler, G. H. 2013. Rainforest Ecosystems, Animal Diversity. In *Encyclopedia of Biodiversity (Second Edition)*, 304–312. Academic Press.

Aleixo, I., D. Norris, L. Hemerik, A. Barbosa, E. Prata, F. Costa, and L. Poorter. 2019. Amazonian rainforest tree mortality driven by climate and functional traits. *Nature Climate Change* 9: 384–388. doi:10.1038/s41558-019-0458-0.

Blundo, C., J. Carilla, R. Grau, A. Malizia, L. Malizia, O. Osinaga-Acosta, M. Bird, M. Bradford, et al. 2021. Taking the pulse of Earth's tropical forests using networks of highly distributed plots. *Biological Conservation*: 108849. doi:10.1016/j.biocon.2020.108849.

Braakhekke, M. C., J. C. Doelman, P. Baas, C. Müller, S. Schaphoff, E. Stehfest, and D. P. van Vuuren. 2019. Modeling forest plantations for carbon uptake with the LPJmL dynamic global vegetation model. *Earth System Dynamics* 10: 617–630. doi:10.5194/esd-10-617-2019.

Brienen, R. J. W., O. L. Phillips, T. R. Feldpausch, E. Gloor, T. R. Baker, J. Lloyd, G. Lopez-Gonzalez, A. Monteagudo-Mendoza, et al. 2015. Long-term decline of the Amazon carbon sink. *Nature* 519: 344–348. doi:10.1038/nature14283.

Chave, J., B. Riéra, and M.-A. Dubois. 2001. Estimation of Biomass in a Neotropical Forest of French Guiana: Spatial and Temporal Variability. *Journal of Tropical Ecology* 17: 79–96.

Chung, S.-W., F. L. Miles, R. A. Sikes, C. R. Cooper, M. C. Farach-Carson, and B. A. Ogunnaike. 2009. Quantitative Modeling and Analysis of the Transforming Growth Factor β Signaling Pathway. *Biophysical Journal* 96: 1733–1750. doi:10.1016/j.bpj.2008.11.050.

Condit, R., S. P. Hubbell, and R. B. Foster. 1995. Mortality Rates of 205 Neotropical Tree and Shrub Species and the Impact of a Severe Drought. *Ecological Monographs* 65: 419–439. doi:10.2307/2963497.

Cramer, W., A. Bondeau, S. Schaphoff, W. Lucht, B. Smith, and S. Sitch. 2004. Tropical forests and the global carbon cycle: impacts of atmospheric carbon dioxide, climate change and rate of deforestation. Edited by Y. Malhi. *Philosophical Transactions of the Royal Society of London. Series B: Biological Sciences* 359: 331–343. doi:10.1098/rstb.2003.1428.

Duru, M., M. Adam, P. Cruz, G. Martin, P. Ansquer, C. Ducourtieux, C. Jouany, J. P. Theau, et al. 2009. Modelling above-ground herbage mass for a wide range of grassland community types. *Ecological Modelling* 220: 209–225. doi:10.1016/j.ecolmodel.2008.09.015.

FAO. 2012. *Global ecological zones for FAO forest reporting: 2010 Update*. Forest Resources Assessment Working Paper 179. Rome.

FAO and UNEP. 2020. *The State of the World's Forests 2020. Forests, biodiversity and people*. Rome.

Farrior, C. E., S. A. Bohlman, S. Hubbell, and S. W. Pacala. 2016. Dominance of the suppressed: Power-law size structure in tropical forests. *Science* 351: 155–157. doi:10.1126/science.aad0592.

Fichtler, E., D. A. Clark, and M. Worbes. 2003. Age and Long-term Growth of Trees in an Old-growth Tropical Rain Forest, Based on Analyses of Tree Rings and 14C. *Biotropica* 35: 306–317.

Herwitz, S. R., R. E. Slye, and S. M. Turton. 2000. Long-Term Survivorship and Crown Area Dynamics of Tropical Rain Forest Canopy Trees. *Ecology* 81: 585–597. doi:10.1890/0012-9658(2000)081[0585:LTSACA]2.0.CO;2.

Hou, T., Y. Zhu, H. Lü, E. Sudicky, Z. Yu, and F. Ouyang. 2015. Parameter sensitivity analysis and optimization of Noah land surface model with field measurements from Huaihe River Basin, China. *Stochastic Environmental Research and Risk Assessment* 29: 1383–1401. doi:10.1007/s00477-015-1033-5.

Hubau, W., S. L. Lewis, O. L. Phillips, K. Affum-Baffoe, H. Beeckman, A. Cuní-Sanchez, A. K. Daniels, C. E. N. Ewango, et al. 2020. Asynchronous carbon sink saturation in African and Amazonian tropical forests. *Nature* 579: 80–87. doi:10.1038/s41586-020-2035-0.

Kohyama, T., E. Suzuki, T. Partomihardjo, T. Yamada, and T. Kubo. 2003. Tree species differentiation in growth, recruitment and allometry in relation to maximum height in a Bornean mixed dipterocarp forest. *Journal of Ecology* 91: 797–806. doi:10.1046/j.1365-2745.2003.00810.x.

Kuntoro, A. A., A. Wahyu, and T. Yamashita. 2009. The Effect of Deforestation on Regional Terrestrial Carbon Balance: A Case Study of Borneo Island. *Journal of International Development and Cooperation* 15: 141–165.

Le Quéré, C., R. M. Andrew, J. G. Canadell, S. Sitch, J. I. Korsbakken, G. P. Peters, A. C. Manning, T. A. Boden, et al. 2016. Global Carbon Budget 2016. *Earth System Science Data* 8: 605–649. doi:10.5194/essd-8-605-2016.

Locosselli, G. M., R. J. W. Brienen, M. de S. Leite, M. Gloor, S. Krottenthaler, A. A. de Oliveira, J. Barichivich, D. Anhuf, et al. 2020. Global tree-ring analysis reveals rapid decrease in tropical tree longevity with temperature. *Proceedings of the National Academy of Sciences* 117: 33358–33364. doi:10.1073/pnas.2003873117.

Malhi, Y., C. Doughty, and D. Galbraith. 2011. The allocation of ecosystem net primary productivity in tropical forests. *Philosophical Transactions of the Royal Society B: Biological Sciences* 366: 3225–3245. doi:10.1098/rstb.2011.0062.

Mitchard, E. T. A. 2018. The tropical forest carbon cycle and climate change. *Nature* 559: 527–534. doi:10.1038/s41586-018-0300-2.

Muller-Landau, H. C., R. S. Condit, K. E. Harms, C. O. Marks, S. C. Thomas, S. Bunyavejchewin, G. Chuyong, L. Co, et al. 2006. Comparing tropical forest tree size distributions with the predictions of metabolic ecology and equilibrium models. *Ecology Letters* 9: 589–602. doi:10.1111/j.1461-0248.2006.00915.x.

Nair, K. K. N. 2004. Tropical forests | Monsoon Forests (Southern and Southeast Asia). In *Encyclopedia of Forest Sciences*, 1752–1762. Elsevier.

Ngoma, J., M. C. Braakhekke, B. Kruijt, E. Moors, I. Supit, J. H. Speer, R. Vinya, and R. Leemans. 2019. Modelling the response of net primary productivity of the Zambezi teak forests to climate change along a rainfall gradient in Zambia. *Biogeosciences* 16: 3853–3867. doi:10.5194/bg-16-3853-2019.

Nias, R. C. 2013. Endangered Ecosystems. In *Encyclopedia of Biodiversity*, 169–175. Elsevier. doi:10.1016/B978-0-12-384719-5.00257-4.

Ostle, N. J., P. Smith, R. Fisher, F. Ian Woodward, J. B. Fisher, J. U. Smith, D. Galbraith, P. Levy, et al. 2009. Integrating plant-soil interactions into global carbon cycle models. *Journal of Ecology* 97: 851–863. doi:10.1111/j.1365-2745.2009.01547.x.

Pan, Y., R. A. Birdsey, J. Fang, R. Houghton, P. E. Kauppi, W. A. Kurz, O. L. Phillips, A. Shvidenko, et al. 2011. A Large and Persistent Carbon Sink in the World's Forests. *Science* 333: 988–993. doi:10.1126/science.1201609.

Pappas, C., S. Fatichi, S. Leuzinger, A. Wolf, and P. Burlando. 2013. Sensitivity analysis of a process-based ecosystem model: Pinpointing parameterization and structural issues: *Journal of Geophysical Research: Biogeosciences* 118: 505–528. doi:10.1002/jgrg.20035.

Pavurala, N., and L. E. K. Achenie. 2013. A mechanistic approach for modeling oral drug delivery. *Computers & Chemical Engineering* 57: 196–206. doi:10.1016/j.compchemeng.2013.06.002.

Penman, J., M. Gytarsky, T. Hiraishi, T. Krug, D. Kruger, R. Pipatti, L. Buendia, K. Miwa, et al., ed. 2003. *Good practice guidance for land use, land-use change and forestry*. Kanagawa, Japan.

Phillips, O. L., Y. Malhi, N. Higuchi, W. F. Laurance, P. Núñez, R. M. Vásquez, S. G. Laurance, L. V. Ferreira, et al. 1998. Changes in the Carbon Balance of Tropical Forests: Evidence from Long-Term Plots. *Science* 282: 439–442. doi:10.1126/science.282.5388.439.

Phillips, O. L., G. van der Heijden, S. L. Lewis, G. López-González, L. E. O. C. Aragão, J. Lloyd, Y. Malhi, A. Monteagudo, et al. 2010. Drought-mortality relationships for tropical forests. *New Phytologist* 187: 631–646. doi:10.1111/j.1469-8137.2010.03359.x.

Phillips, O. L., M. J. P. Sullivan, T. R. Baker, A. Monteagudo Mendoza, P. N. Vargas, and R. Vásquez. 2019. Species Matter: Wood Density Influences Tropical Forest Biomass at Multiple Scales. *Surveys in Geophysics* 40: 913–935. doi:10.1007/s10712-019-09540-0.

Pillet, M., E. Joetzjer, C. Belmin, J. Chave, P. Ciais, A. Dourdain, M. Evans, B. Hérault, et al. 2018. Disentangling competitive vs. climatic drivers of tropical forest mortality. Edited by Shurong Zhou. *Journal of Ecology* 106: 1165–1179. doi:10.1111/1365-2745.12876.

Pugh, T. A. M., T. Rademacher, S. L. Shafer, J. Steinkamp, J. Barichivich, B. Beckage, V. Haverd, A. Harper, et al. 2020. Understanding the uncertainty in global forest carbon turnover. *Biogeosciences* 17: 3961–3989. doi:10.5194/bg-17-3961-2020.

Reyes, G., S. Brown, J. Chapman, and A. E. Lugo. 1992. *Wood densities of tropical tree species*. Gen. Tech. Rep. SO-88. New Orleans, LA: U.S.: Department of Agriculture, Forest Service, Southern Forest Experiment Station.

Saatchi, S. S., N. L. Harris, S. Brown, M. Lefsky, E. T. A. Mitchard, W. Salas, B. R. Zutta, W. Buermann, et al. 2011. Benchmark map of forest carbon stocks in tropical regions across three continents. *Proceedings of the National Academy of Sciences* 108: 9899–9904. doi:10.1073/pnas.1019576108.

Sabah Forestry Department. 2013. *Annual report 2012*. Sandakan: Sabah Forestry Department.

Seiler, C. 2014. The Sensitivity of Tropical Forests to Climate Variability and Change in Bolivia. PhD, Wageningen, The Netherlands: Wageningen University.

Seiler, C., R. W. A. Hutjes, B. Kruijt, and T. Hickler. 2015. The sensitivity of wet and dry tropical forests to climate change in Bolivia. *Journal of Geophysical Research: Biogeosciences* 120: 399–413. doi:10.1002/2014JG002749.

Smith, B. n.d. LPJ-GUESS - an ecosystem modelling framework.

Smith, B., I. C. Prentice, and M. T. Sykes. 2001. Representation of vegetation dynamics in the modelling of terrestrial ecosystems: comparing two contrasting approaches within European climate space: *Global Ecology and Biogeography* 10: 621–637. doi:10.1046/j.1466-822X.2001.t01-1-00256.x.

Smith, B., D. Wårlind, A. Arneth, T. Hickler, P. Leadley, J. Siltberg, and S. Zaehle. 2014. Implications of incorporating N cycling and N limitations on primary production in an individual-based dynamic vegetation model. *Biogeosciences* 11: 2027–2054. doi:10.5194/bg-11-2027-2014.

de Sousa, L. M., L. Poggio, N. H. Batjes, G. B. M. Heuvelink, B. Kempen, E. Riberio, and D. Rossiter. 2020. *SoilGrids 2.0: producing quality-assessed soil information for theglobe*. Preprint. Soils and the natural environment. doi:10.5194/soil-2020-65.

Stephenson, N. L., A. J. Das, R. Condit, S. E. Russo, P. J. Baker, N. G. Beckman, D. A. Coomes, E. R. Lines, et al. 2014. Rate of tree carbon accumulation increases continuously with tree size. *Nature* 507: 90–93. doi:10.1038/nature12914.

TEAM Network. 2021. https://www.wildlifeinsights.org/team-network. Accessed May 24.

TreeMort. 2021. https://more.bham.ac.uk/treemort/. Accessed May 24.

Westoby, M. 1984. The Self-Thinning Rule. In *Advances in Ecological Research*, 14:167–225. Elsevier. doi:10.1016/S0065-2504(08)60171-3.

Worbes, M., and W. J. Junk. 1999. How old are tropical trees? The persistence of a myth. *IAWA Journal* 20: 255–260.

Zhou, X., Y. Fu, L. Zhou, B. Li, and Y. Luo. 2013. An imperative need for global change research in tropical forests. *Tree Physiology* 33: 903–912. doi:10.1093/treephys/tpt064.

A Appendix – Justification of npatch(100)

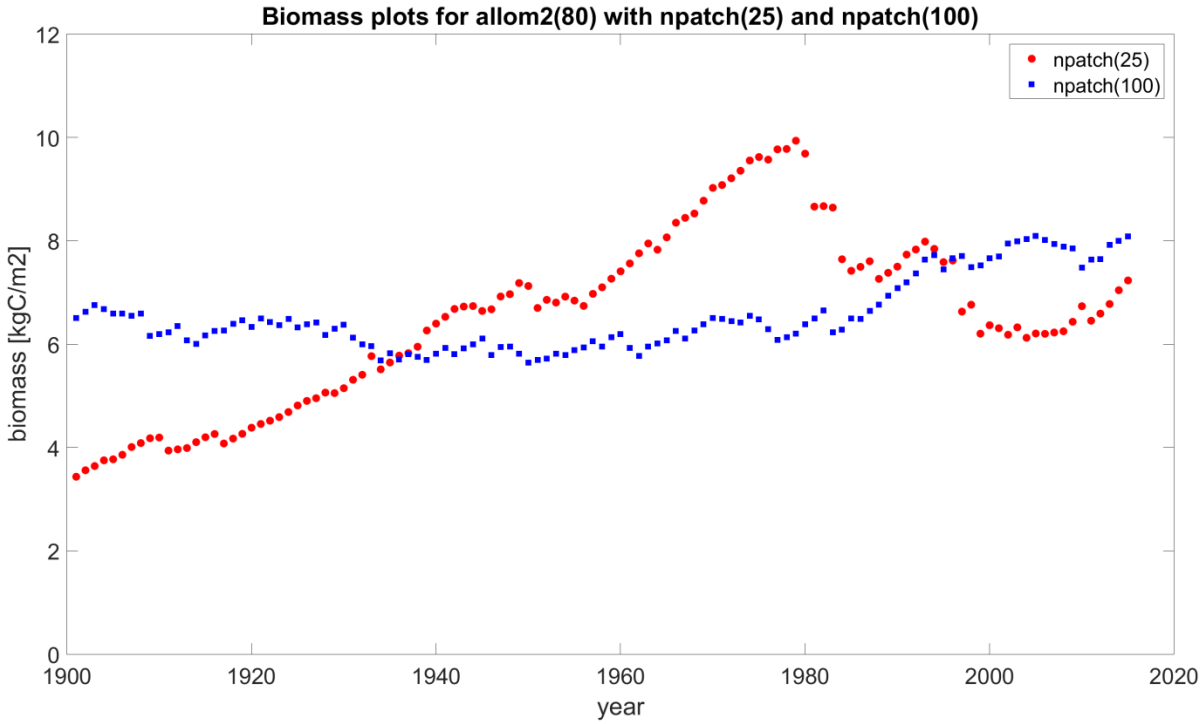

Figure A. Plot showing the stored biomass at COG simulated using 25 patches and 100 patches, respectively. The latter resulted in a more stable output with fewer abrupt changes, for example around 1980.

B Appendix – Tree density vs. large tree biomass

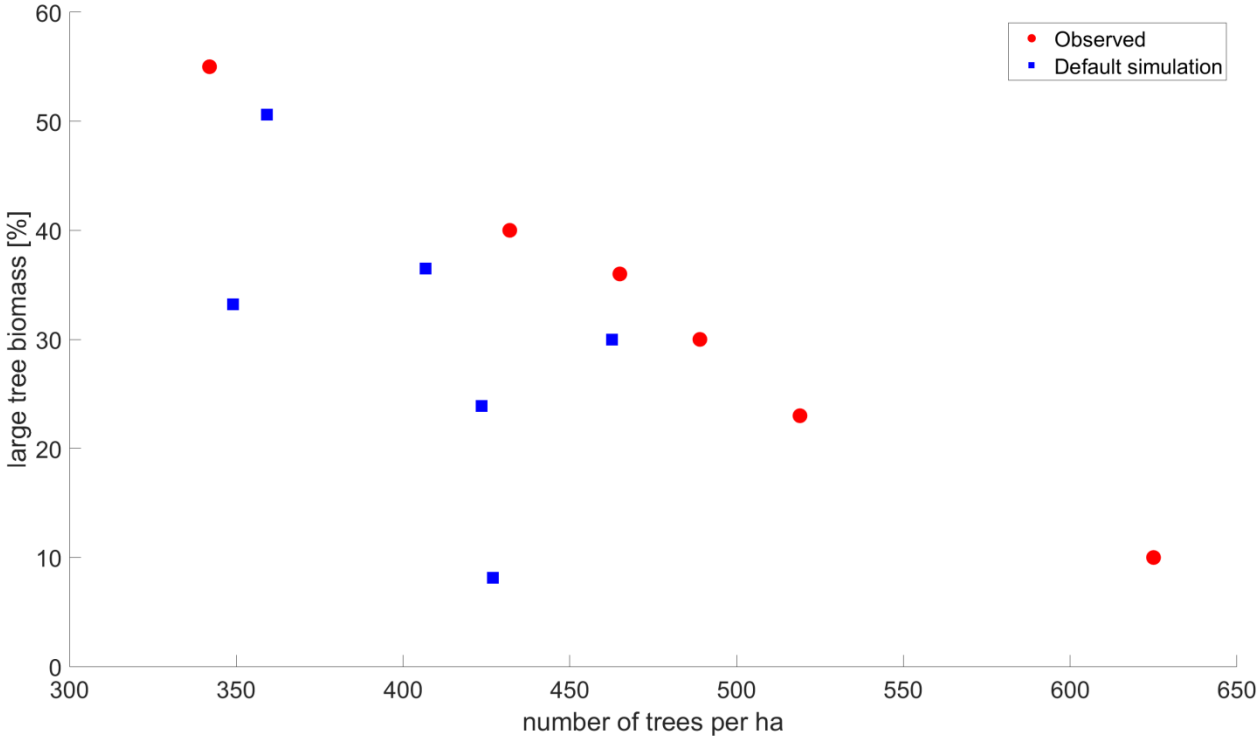

Figure B. Tree density in number of trees per hectare against biomass accounted for by large trees as a percentage of the total biomass. Each dot refers to the output at one of the six sites where the red dots indicate the validation data and the blue dots show the results from the default simulation.